Available online at www.sciencedirect.com
ScienceDirect
C. R. Physique 9 (2008) 262–275
COMPTES RENDUS PHYSIQUE
http://france.elsevier.com/direct/COMREN/

Recent developments in terahertz optoelectronics/Développements récents en optoélectronique térahertz

Continuous-wave terahertz by photomixing: applications to gas phase pollutant detection and quantification

Francis Hindle *, Arnaud Cuisset, Robin Bocquet, Gaël Mouret

Laboratoire de physico-chimie de l'atmosphère, UMR CNRS 8101, Université du Littoral Côte d'Opale, 189A, avenue Maurice-Schumann, 59140 Dunkerque, France

Available online 19 November 2007

Abstract

Recent advances in the development of monochromatic continuous-wave terahertz sources suitable for high resolution gas phase spectroscopy and pollution monitoring are reviewed. Details of a source using an ultra fast opto-electronic photomixing element are presented. The construction of a terahertz spectrometer using this source has allowed spectroscopic characterisation and application studies to be completed. Analysis of H_2S and OCS under laboratory conditions are used to demonstrate the spectrometer performance, and the determination of the transition line strengths and pressure self broadening coefficients for pure rotational transitions of OCS. The spectral purity 5 MHz, tunability 0.3 to 3 THz, and long wavelength ≈200 μm of this source have been exploited to identify and quantify numerous chemical species in cigarette smoke. The key advantages of this frequency domain are its high species selectivity and the possibility to make reliable measurements of gas phase samples heavily contaminated by aerosols and particles. ***To cite this article: F. Hindle et al., C. R. Physique 9 (2008).***

Résumé

Ondes continues térahertz par système de photomélange : applications à la detection et à la quantification des gaz polluants. Cet article résume les récentes avancées dans le développement de sources monochromatiques et continues d'ondes térahertz utilisées dans des expériences de spectroscopie à haute résolution en phase gazeuse, consacrées à la métrologie de polluants. Les caractéristiques d'une source optoélectronique employant un photomélangeur ultrarapide sont détaillées ainsi que son emploi dans la réalisation d'un spectromètre térahertz utilisé dans diverses applications spectroscopiques. L'analyse de H_2S et OCS a permis d'une part de valider les performances du spectromètre conçu et d'autre part de déterminer des paramètres spectroscopiques tels que les forces de raie et les coefficients d'élargissement par pression associés aux transitions rotationnelles d'OCS. La pureté spectrale (5 MHz), l'accordabilitié de 0,3 à 3 THz et la longueur d'onde importante (≈200 μm) de cette source ont été exploitées pour identifier et quantifier des espèces chimiques dans la fumée de cigarette. Les expériences réalisées tirent avantage du rayonnement térahertz qui offre une haute sélectivité et permet de réaliser des mesures dans des échantillons gazeux largement contaminés par de nombreux aérosols et particules. ***Pour citer cet article : F. Hindle et al., C. R. Physique 9 (2008).***

Keywords: Terahertz; Gas phase pollutants

Mots-clés : Térahertz ; Gaz polluants

* Corresponding author.
E-mail address: francis.hindle@univ-littoral.fr (F. Hindle).

1631-0705/$ – see front matter
doi:10.1016/j.crhy.2007.07.009

1. Introduction

1.1. Terahertz technology

The terahertz (THz) frequency domain is situated at the high frequency side of the microwave band and at the low frequency side of the infrared band. The domain is often defined to cover the frequencies from 0.3 to 10 THz corresponding to the submillimeter wavelengths from 1 mm to 30 μm. This region holds the promise of a large quantity of information as it is particularly rich in molecular resonances. The technological difficulties in the development of powerful, tunable, monochromatic sources in the terahertz waveband have with no doubt hindered its exploitation. Techniques that are capable of directly producing THz radiation are in competition with frequency conversion techniques which approach from both the electronic or lower frequencies and the optical or higher frequencies.

Direct sources that have demonstrated their utility for spectroscopic based applications include carcinotrons, molecular lasers and relativistic electron sources. Carcinotron or Backward Wave Oscillator (BWO) sources [1,2] can operate at frequencies between 180 and 1500 GHz providing a minimum power in the order of 1 mW. Their spectral purity is also very attractive, permitting a spectrometer resolution of as little as 50 kHz to be achieved. The shortcomings of these sources lie in their fabrication and operation which remain particularly costly providing devices with relatively short lifetimes. Their commercial availability is also problematic presently only being supplied by a single Russian manufacturer. A number of devices are required in order to cover the complete frequency range.

A more reliable source can be obtained by the use of a molecular laser pumped by a high power CO_2 laser, allowing fixed THz wavelengths to be generated. For spectroscopy applications, frequency stabilisation of both lasers is desirable. A tunability can then be obtained by mixing the THz laser radiation with a second frequency source in a Schottky diode to generate tunable sidebands, typically producing several μW of useful power. The use of a standard commercially available microwave synthesizer allows frequencies at up to 20 GHz from the laser line to be accessed and permits a heterodyne detection scheme to be employed [3]. This method can only cover a relatively small waveband around the molecular laser frequency, however, the use of a variety of molecules gives access to approximately 50% of the THz domain [4,5]. The tuning range of this technique can be extended by employing higher frequency secondary sources such as klystrons or even carcinotrons which unfortunately necessitate the use of bolometric detection and the suppression of one sideband and the fundamental laser line. This solution increases the coverage to around 95% [6].

Relativistic electron sources such as synchrotrons and free electrons lasers may be considered as the ultimate THz source as they are perfectly tunable and are capable providing intense radiation over the entire frequency range. These installations are, however, extremely costly and by their nature they remain the reserve national or international scientific programs [7,8].

The development of Quantum Cascade Lasers (QCL) holds promise of further choice in this category. They are capable of operating at the high frequency end of the THz waveband and even down to 2 THz at which frequency cryogenic cooling is required for continuous wave (CW) operation. Their principle drawback is the limited tuning range ≈4 GHz, however devices delivering 6 mW of power with a linewidth in the order of 0.5 MHz (integration time = 300 ms) have demonstrated their utility for spectroscopy [9].

To overcome the technological limitations of such direct sources, methods to convert power from spectral regions where generation is easier are often used. The considerable progress realised in the elaboration of non-linear crystals and semiconductors, particularly ultrafast devices using Low Temperature Grown GaAs (LTG-GaAs), have permitted significant advances in the development of optically based THz sources. The use of LTG-GaAs and ultrashort optical pulses can produce broadband THz radiation pulses. Time Domain Spectroscopy (TDS) experiments have extensively employed such a source providing a useful method to study absorption and dispersion of various samples in the THz frequency range [10–14]. Properties of dielectrics, semiconductors, gas, liquid and flames have been studied by THz-TDS which presents a wide spectral coverage, 0.3 to 3 THz, however the spectral resolution is limited to the order of 1 GHz. Commercial instruments for THz spectroscopy and imaging based on this source are now a viable proposition [15–17].

Up conversion, or the harmonic generation from microwaves sources has been successfully exploited for many years [18–20]. A klystron with a frequency range of 20 to 150 GHz or BWO [21] may be used as the fundamental source with harmonic generation resulting from the non-linearity of a component such as a Schottky diode. The avail-

able power rapidly decreases at high frequency, however this type of system is commercially available and can provide around 100 mW at 1 THz [22].

An alternative possibility is the down conversion of two laser oscillators, CO_2 or Titanium–Sapphire (Ti:Sa) or Ti:Al_2O_3 lasers can be employed for this technique. The discrete emission lines of the gas laser results in a source with relatively stable frequency emission that, however, can not be continuously tuned. In comparison the broad gain profile of the Ti:Sa crystal permits continuous tuning but requires more complex frequency stabilisation. Terahertz radiation can be produced by the mixing of two CO_2 lasers on a metal–insulator–metal (MIM) diode with the difference frequency corresponding to the required THz frequency, a tunable emission is obtained by including a microwave frequency in the mixing stage. This solution presently offers the greatest degree of tunability available and has been extensively used in absolute frequency measurements [23,24]. The MIM diodes consist of thin metallic wire with a fine etched tip in weak contact with an oxidized metallic surface. The principal drawbacks of the MIM diodes are the reproducibility of the electrical characteristics of the contact points and poor mechanical stability.

Photomixing or optical heterodyning is a down conversion technique. The two lasers with a difference frequency corresponding to the THz frequency required are spatially overlapped and focused onto the semiconductor material which is subjected to an electric field. The photonic absorption induces a conductivity variation and corresponding current. The ultra-rapid electronic response of the LTG GaAs ($\approx$500 fs) permits the intermediate or difference frequency component to be converted into THz radiation via radiating elements, which may be broadband log spiral or dipole antennae. Hence a continuous wave THz (CW-THz) source is obtained. Free space THz photomixing using a LTG-GaAs mixer was first demonstrated by Brown et al. in 1995 to generate radiation at frequencies up to 3.8 THz [25,26]. This THz source was subsequently used to study SO_2 self-broadening at frequencies lower than 1 THz. The maximum frequency of this study was limited to 1000 GHz due to a poor signal to noise ratio of the photomixer element used [27]. More recently Ito et al. [28] demonstrated UniTravelling-Carrier (UTC) photodiodes producing more than 10 μW of power at 1 THz with a resonant antenna and 2 μW with a broadband antenna.

Also in this category is the elegant proposition made by Goyette et al. [29], monochromatic tunable CW-THz was to be obtained by the elimination of all but a single component of the frequency comb of a femtosecond THz pulse. This team successfully demonstrated the use of this approach to measure a transition of carbonyl sulphide (OCS) at 340 GHz.

1.2. High resolution gas phase spectroscopy

The THz domain allows rotational transitions of light polar molecules and low frequency vibrational modes of larger molecular systems to be probed. Small molecules such hydrogen sulphide (H_2S), OCS, formaldehyde (H_2CO) and ammonia (NH_3), present an interest as an atmospheric pollutant and are ideal candidates for THz spectroscopy because they possess intense transitions in this frequency domain. Larger molecules such as methanol (CH_3OH), toluene (C_7H_8) and acetone (C_3H_6O) have been less exhaustively studied due to the internal rotation of the molecules producing many overlapping transitions which can not be fully resolved with the spectral resolution of existing spectrometers. The skeletal deformation of polycyclic aromatic hydrocarbons (PAH) [30] and large amplitude motions of bio-molecules can also be examined in the THz domain but require a spectrometer with high sensitivity. The analysis of gas phase samples requires a spectral resolution well suited to the high quality factor of the resonances with the molecules in the gas phase at atmospheric pressure and at very low pressure. Taking the example of OCS, the most abundant tropospheric pollutant, its Doppler linewidth contribution is in the order of $\Delta\nu/\nu \approx 10^{-6}$ (HWHM = 0.8 MHz at 1 THz and ambient temperature) whereas the collisional self-broadening is 5.7 MHz/mbar. Hence a spectral resolution of 1 MHz is sufficient for the quantification of OCS or similar species at pressures in the excess 3 mbar where the spectral broadening is dominated by molecular collisions. The attraction of optical down conversion over other alternative THz sources for spectroscopic applications is the degree of tunability which offers continuous coverage from 100 GHz to 3 THz at reasonable intensity levels for exploitation with bolometric detection.

At present only a small number of laboratories are able to undertake such studies. A team at the National Institute of Standards and Technology have measured self broadening widths and pressure induced shifts of several purely rotational water vapor lines in the frequency range 0.4 to 1.73 THz using a CW-THz photomixing spectrometer with a resolution in the order of $\approx 10^{-4}$ cm^{-1} or 3 MHz [31]. Also in the field of astrophysics Chen et al. at the Jet Propulsion Laboratory have used a solid state (Ti:Sa lasers replaced by diode lasers) CW-THz photomixing spectrometer to study the ro-vibrational spectrum of Ammonia including the measurement of transition frequencies and pressure

induced shifts. This solution provides an improved spectral accuracy of 230 kHz at the cost of considerable additional complexity [32].

2. Continuous-Wave Terahertz spectrometer

The CW-THz spectrometer developed at the Laboratoire de Physico-Chimie de l'Atmosphère may be divided into the following functional units: two visible lasers (ω_1 and ω_2), a laser frequency stabilisation/control system, means of spatially overlapping the visible laser beams, the photomixer element, a THz beam propagation path including sample chamber and a detector, see Fig. 1. The commercial availability of frequency stabilised Ti:Sa lasers together the necessary frequency measurement and control systems make them a versatile candidate for the laboratory development of CW-THz sources. The CW-THz spectrometer for gas phase subjects used two Ti:Sa (Coherent, Autoscan 899-29) pumped by individual Nd:YVO_4 doubled solid state lasers (Coherent, Verdi V-10). The use of two different mirror sets in the Ti:Sa lasers provides a tuning ranges of 690 to 840 nm and 780 to 930 nm with a power in the order of 1 W and a spectral purity of around 2 MHz. An estimation of the spectral resolution of the optical beat signal was measured with a difference frequency within the bandwidth of a fast photodiode and spectrum analyser, yielding a FWHM of 5 MHz with an integration time of 5 ms.

The correct collimation and propagation of the THz beam is critical in order to permit a sufficient interaction length and conserve adequate power. The first obstacle is large divergence of the THz beam and the high refractive index of the semiconductor photomixer which necessitate the use of a semi-hemispherical silicon lens immediately after the photomixer. After the silicon lens the THz beam is collimated by a metallic off-axis parabolic mirror and subsequently propagated through the sample chamber. At the exit of the sample chamber an identical parabolic mirror is used to focus the entire beam onto a detecting element.

2.1. Photomixing

In order to generate continuous wave THz radiation by photomixing, two lasers with a THz frequency separation and with identical polarisations are spatially overlapped either in free space or by means of fibre optic coupler. The co-linear beams are subsequently focused within a region of a LTG-GaAs semiconductor which is subjected to a electric field by an interdigitated electrode array of typical dimensions 8×8 μm^2. The photomixer devices for this application where developed and fabricated as part of a collaboration with the Institut d'électronique de microélectronique et de nanotechnologie (IEMN) [33], Lille France. They consist of GaAs substrate on which a 1 μm layer LTG-GaAs

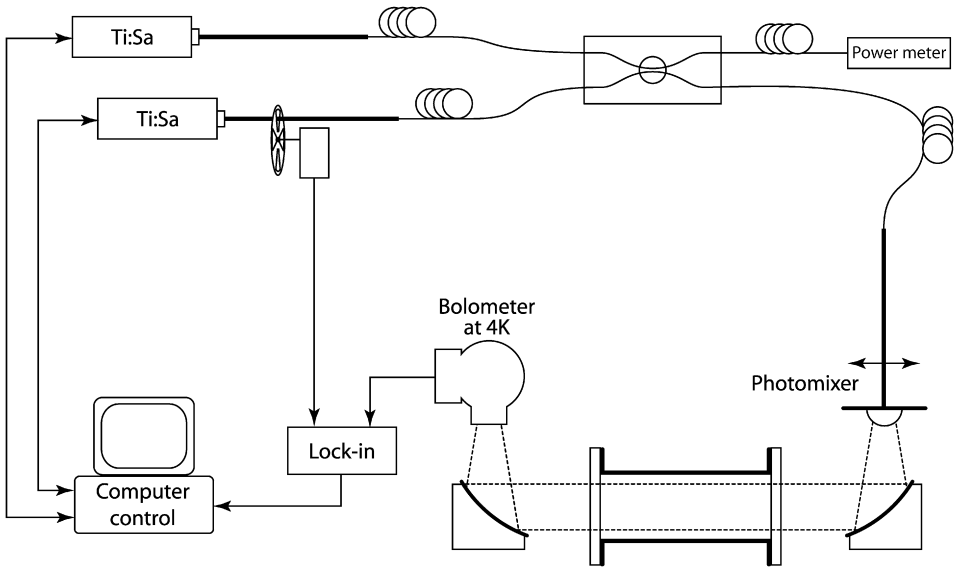

Fig. 1. Schematic diagram of CW-THz spectrometer.

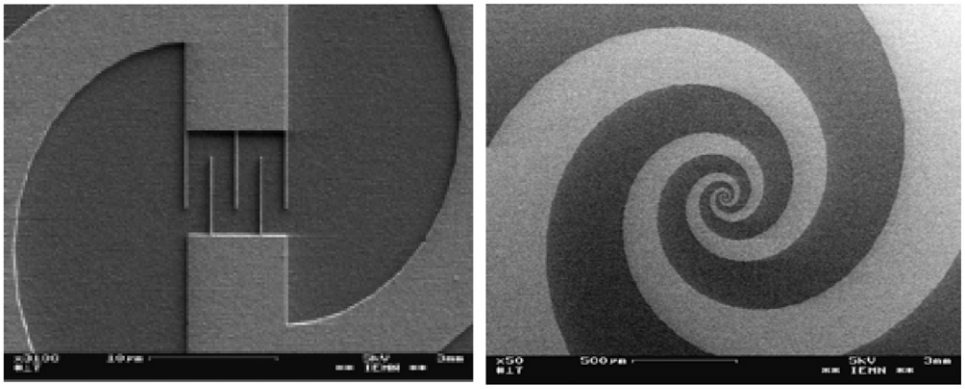

(a) (b)

Fig. 2. (a) Interdigitated electrode array at the centre of the photomixer device, dimension of $8 \times 8\ \mu m^2$. (b) Spiral antennae coupled to electrode array, maximum radius of 1.5 mm. Images provided by IEMN.

is deposited by molecular beam epitaxy at a temperature of 300 °C. The electrode array and radiating antenna are fabricated from a metal layer patterned using electron beam lithography. An electromicrograph of the photomixing is presented in Fig. 2. Photonic absorption by the semiconductor stimulates an increase in the charge carrier density which is a function of the instantaneous optical power and the semiconductor charge carrier lifetime, τ. In the case of LTG-GaAs, lifetimes in the order of 500 fs may be routinely obtained and permit difference frequencies in the THz domain to be converted into current i_{THz} by means of an applied electric field. The current is coupled to a log spiral antenna directly connected to the electrode array. The THz radiation power emitted by the antenna is dependent on the incident laser powers P_1 and P_2, the electrode array bias voltage V_{BIAS}, the charge carrier lifetime τ, the antenna R and C values, and the difference frequency $w_1 - w_2 = w_{\mathrm{THz}}$, see Eq. (1).

$$P_{\mathrm{THz}} \propto \frac{V_{\mathrm{BIAS}}^2 (P_1 + P_2)^2 R}{(1 + w_{\mathrm{THz}}^2 \tau^2).(1 + w_{\mathrm{THz}}^2 R^2 C^2)} \tag{1}$$

The intensity of the THz radiation typically produced by the standard spiral photomixers described above is in the order of 100 nW at frequencies below the cut off (550 GHz) for a device with $8 \times 8\ \mu m^2$ electrode array and carrier lifetime of 340 fs, see Fig. 3. At higher frequency the response falls at a rate of 40 dB/decade. The maximum emission is limited by the breakdown voltage of the electrode array and the thermal management of the GaAs substrate. In order to examine the performance of alternative photomixer structures, a small number of devices with a transversal electrode configuration [34] were developed as part of a collaboration with the IEMN. The device consists of one electrode and associated arm of the spiral on the first surface of the LTG-GaAs layer with the other electrode and spiral being on opposite surface. An emission enhancement is obtained providing 1 μW of emission below the cut off frequency as a result of the increased volume of the active region.

2.2. Detectors

In this waveband the choice of sensitive incoherent detectors is limited to cryogenically cooled bolometric systems with either silicon crystal or InSb sensing elements. The silicon detectors allows frequencies in the range 150 GHz to 15 THz to be accessed but have a temporal response of around 1 ms, whereas the InSb element has a response time in the order of 1 μs but its sensitivity decreases rapidly above 500 GHz. Both detectors have a noise equivalent power (NEP) in the order of $1 \times 10^{-12}\mathrm{W\,Hz^{-1/2}}$. The desired THz signal is separated from the thermal background by the modulation of one of the optical lasers and the recovery from the bolometer signal by a lock-in amplifier. The minimum detectable absorption available is most simply expressed in terms of dynamic range DR and is dependent on the detector NEP, the measurement bandwidth Δf, the interaction length L and the THz power P_o:

$$\alpha_{\min} = \frac{1}{L} \ln\left(\frac{P_o}{P_o - NEP\sqrt{\Delta f}}\right) \approx \frac{1}{L.DR} \tag{2}$$

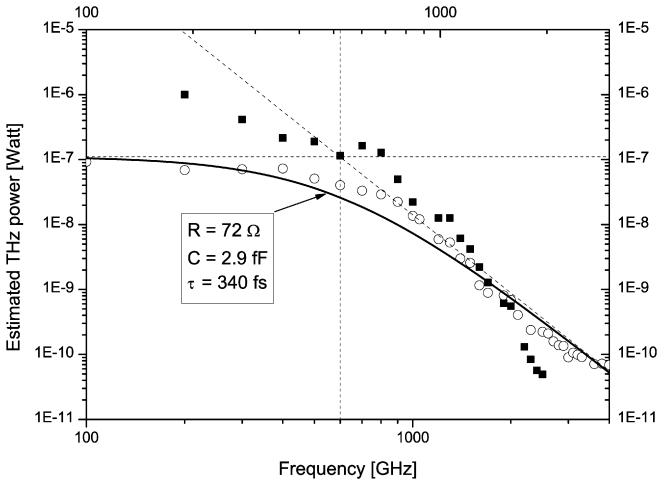

Fig. 3. Spectral response of a LTG-GaAs spiral photomixer with a carrier lifetimes $\tau = 340$ fs (circles) and transversal electrode photomixer (squares).

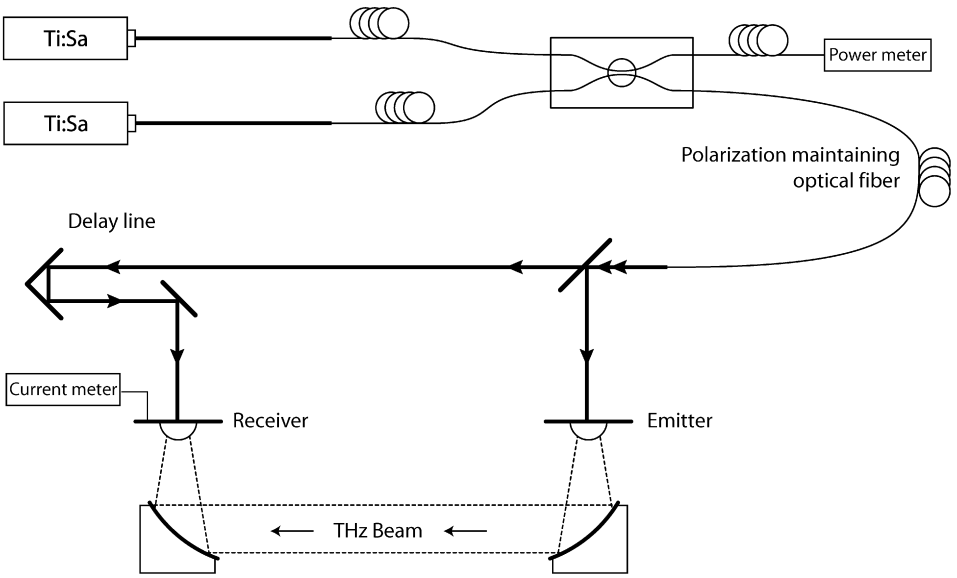

Fig. 4. CW-THz spectrometer with homodyne detection scheme.

where $DR = \frac{P_o}{NEP\sqrt{\Delta f}}$ and $DR \gg 1$.

A coherent or homodyne system may be employed as an alternative to intensity based detectors and uses a second photomixer or a non-linear crystal as the detection element. A fraction of the visible lasers is used in the detector to generate photo-carriers with the THz field being used to accelerate the carriers resulting in the generation of a current to form an electro-optic sampling scheme for the THz field, as illustrated in Fig. 4. As the phase information is retained, the absorption and dispersion of material in the THz path can be obtained. This type of detection not only provides supplementary information compared with incoherent schemes but has the advantage of operating at room temperature. The anomalous dispersion of OCS and the dispersion of Teflon have been measured using this technique [35].

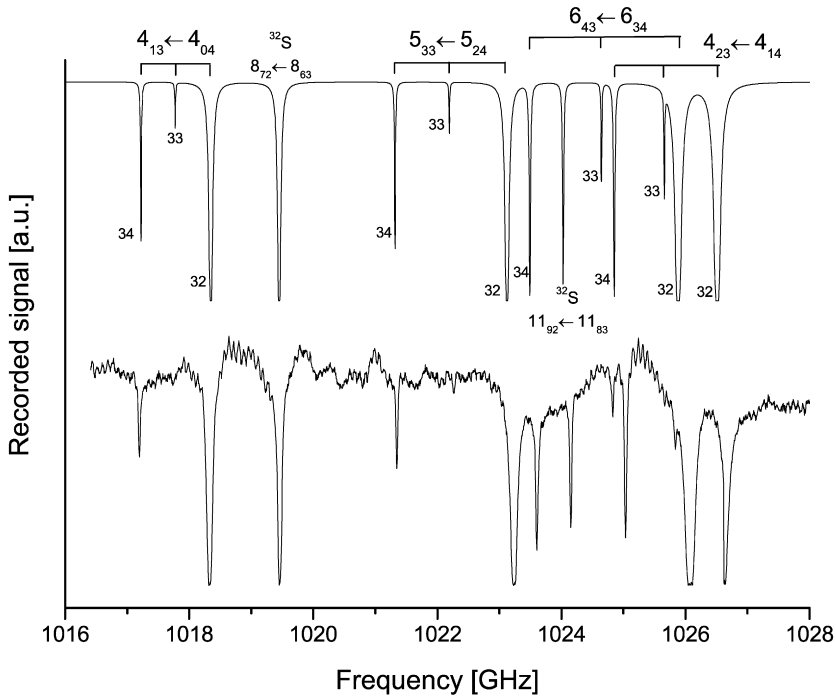

Fig. 5. Measured absorption spectrum of H_2S gas (lower trace) compared with calculated spectrum (upper trace). Pressure 2.5 mbar, $T = 292$ K. Transitions marked with 32, 33 or 34 for isotopologues $H_2\,^{32}S$, $H_2\,^{33}S$ and $H_2\,^{33}S$ respectively.

2.3. Spectrometer tunability and spectral purity

Gaseous Hydrogen Sulphide (H_2S) is emitted by various industries such as petroleum refining, natural gas extraction, waste water treatment and paper production. At the concentration levels above 20 ppm it is toxic, corrosive and cannot be detected by the human nose. This molecule is an ideal candidate for the evaluation of new instruments as it is light, asymmetric and has permanent dipole moment of 0.974 Debye so in the THz region displays many intense purely rotational transitions $J'_{Ka'Kc'} \leftarrow J''_{Ka''Kc''}$ for low J values. The tunability of the spectrometer is demonstrated by the scan illustrated in Fig. 5 which covers a frequency range in excess of 20 GHz. The absorption spectrum of H_2S shows many transitions which are easily attributed and originate from the three sulphur isotopes present in the sample, $H_2\,^{32}S$ (94.9%), $H_2\,^{34}S$ (4.3%), and $H_2\,^{33}S$ (<0.8%). Comparison with the calculated spectrum based on the parameters published in the HITRAN database shows a reasonable agreement with a frequency offset becoming visible at higher frequencies. This is caused by the frequency measurement accuracy which is limited to 200 MHz and slight non-linearity of the scanning mechanism. Although the accuracy is limited the system precision of around 50 MHz is easily improved by frequency calibration to known species to obtain 5 MHz, limited by the stabilisation scheme of the source lasers.

In order to access the spectral purity of the CW-THz source the measurement of a H_2S ($3_{03} \leftarrow 2_{12}$ and $5_{23} \leftarrow 5_{14}$) doublet with a calculated frequency separation of 11.22 MHz was undertaken [36]. A separation of 9 MHz was measured by the spectrometer and the spectrum displayed in Fig. 6 shows that the source purity is easily sufficient to individually resolve the two transitions, this is understood to be the first observation of this doublet. In this case the scanning of the THz frequency was sampled with an interval of 1 MHz. The measurement indicates that the source purity is of this order of magnitude as corroborated by the beatnote measurement.

3. Spectroscopic characterisation

In collaboration with F. Rohart at the Laboratoire de physique des lasers, atomes et molécules (PhLAM) [37] a study of Carbonyl sulphide was undertaken. This molecule was selected as it is the most abundant sulphur compound

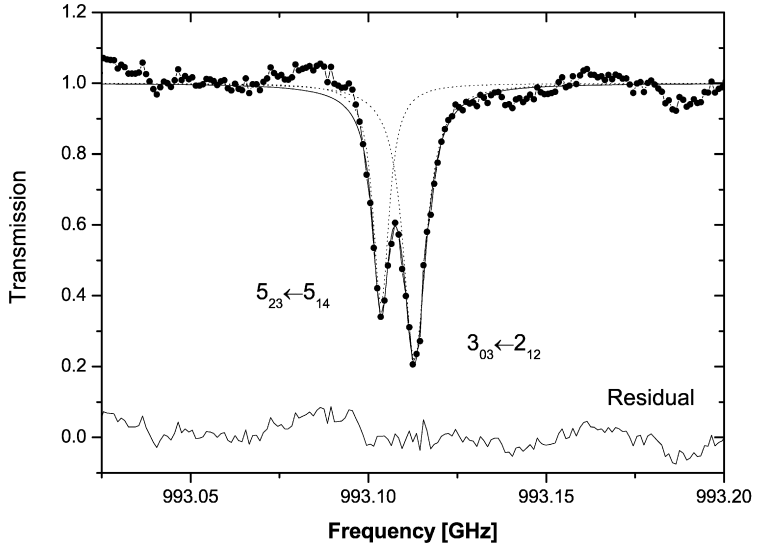

Fig. 6. H_2S doublet, $3_{03} \leftarrow 2_{12}$ and $5_{23} \leftarrow 5_{14}$ ($P = 1.3$ mbar, $T = 292$ K).

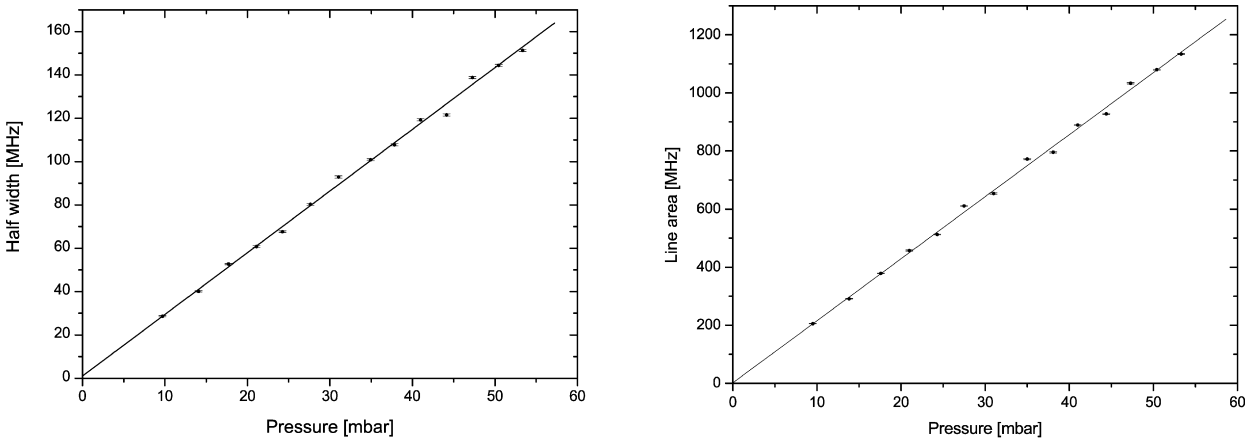

Fig. 7. The (a) linewidth and (b) line area of the $J = 73$ transition of OCS.

found in the troposphere and its simple structure lends itself to the evaluation of spectroscopic techniques. Its characterisation in the THz domain also represents an interest in astrophysics as it has been identified as a component contained in the interstellar medium. This is particularly important in the case of stellar formation which can only be observed in the submillimeter waveband due to the absorption and diffusion of shorter wavelengths caused by clouds of dust particles. A systematic survey was completed to characterise the behaviour of this molecule in the THz domain [38,39], transitions from $J = 10$ (134 GHz) to $J = 90$ (1103 GHz) where measured at pressures from 10 to 50 mbar. Extraction of the line half-width after deconvolution with the instrument response shows a linear dependency with pressure and results in a self-broadening coefficient of 2.84 ± 0.03 GHz bar^{-1}, caused by molecular collisions, see Fig. 7. In a similar manner the line area of the transition can be examined to determine the line intensity, 169.6 ± 3.2 MHz bar^{-1} cm^{-1}. These parameters are critical for the quantification of samples containing an unknown concentration of the target species.

The evolution of the line intensity as a function of J, Fig. 8, was compared with theoretical value [40], good agreement being obtained by leaving the electric dipole moment of OCS as the free parameter in the fitting procedure yielding 0.700 ± 0.014 D compared to 0.7124 ± 0.0002 reported elsewhere [41].

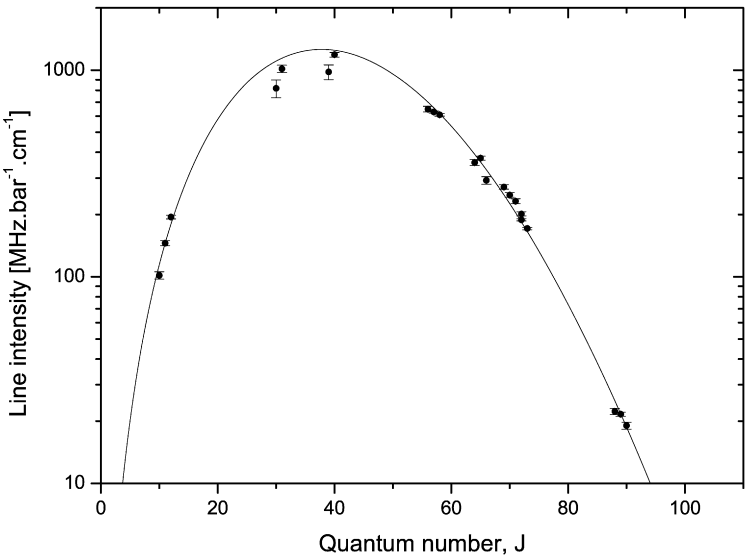

Fig. 8. Line intensity of OCS as function of the quantum number ($T = 292$ K). Experimental data (circles) and fitted function (solid line).

4. Pollution detection

Increasing awareness of exposure to air borne pollution has lead to a greater degree of legislative controls being implemented to limit industrial emission and prevent workers or the public being subjected to potentially hazardous concentration of gas phase species. The detection and quantification of many pollutants presently depends upon classical analytical chemistry techniques which are indirect, species dependent, time consuming, have a poor temporal resolution and often employ one of many capture techniques to obtain the target species in liquid form. Terahertz spectroscopy is an attractive technique for the detection of gas phase pollutants as it offers the potential to provide direct and simultaneous measurements of multiple species from samples contaminated by significant degree of aerosols or particles. In order to demonstrate these capabilities, cigarette smoke was studied as it is a common pollution source which contains a complex mixture of many gaseous compounds and aerosols. The mean particle size aerosols contained in cigarette is in the region of 0.2 μm with typical particle concentrations of 7.2×10^9 particles cm^{-3} [42]. The use of infrared spectroscopy with samples containing such a significant degree of contamination by particles of size approaching the measurement wavelength is likely to be particularly problematic. The minimum wavelength available, 100 μm (3 THz), from the CW-THz source remains at least three orders greater than the size of the aerosols.

4.1. Species identification

In order to identify various gaseous species present in the cigarette smoke, samples were prepared by the aspiration of a burning cigarette with part of the resulting smoke air mixture being retained in the spectrometer sample chamber. Absorption spectra were collected in the range from 600 to 2300 GHz. An individual scan typically of length 100 GHz may contain transitions from multiple species, for example HCN, CO and H_2O lines are clearly visible in the spectrum presented in Fig. 9. The relatively narrow absorption profiles dominated by collisional broadening demonstrate the utility of the good spectral resolution of this spectrometer for simultaneous identification of multiple species. Contributions from moisture in the laboratory environment at atmospheric pressure and water vapour from the tobacco combustion in the sample chamber at 20 mbar are particularly visible for the line at 1322 GHz due to the large difference in collisional broadening.

Unambiguous species identification is dependent on the comparison of multiple observed transition frequencies with the known spectral signature of the pure gaseous species available from published spectroscopy databases or by measurement. In the case of HCN all the $J + 1 \leftarrow J$ transitions from $6 \leqslant J \leqslant 25$ were observed along with the CO transitions $5 \leqslant J \leqslant 19$ other than those coinciding with H_2O transitions, see Table 1. Formaldehyde (H_2CO) was also identified by the observation of the $J'_{\mathrm{Ka'Kc'}} \leftarrow J''_{\mathrm{Ka''Kc''}}$ transitions $14_{1,13} \leftarrow 15_{1,14}$ at 1115.83 GHz, $15_{1,15} \leftarrow 16_{1,16}$

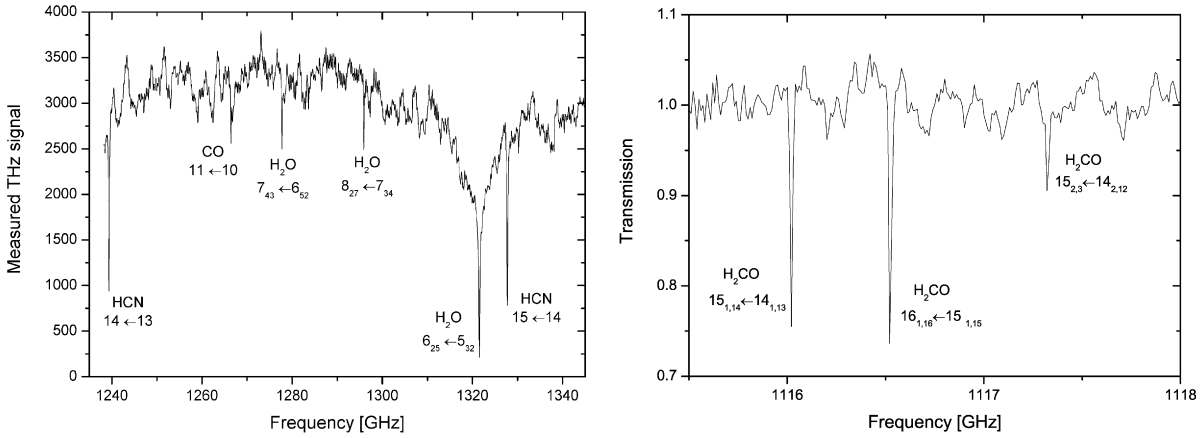

(a) (b)

Fig. 9. (a) Measured spectrum of cigarette smoke containing transitions of HCN, CO and H_2O ($P = 20$ mbar, $T = 294$ K). (b) Transmission spectrum with H_2CO transitions ($P = 0.5$ mbar, $T = 294$ K).

Table 1
Comparison of measured ν_{exp} and published ν_{pub} rotational transition frequencies of HCN and CO [43,44]

HCN transition	ν_{exp} (GHz)	ν_{pub} (GHz)	CO transition	ν_{exp} (GHz)	ν_{pub} (GHz)
$7 \leftarrow 6$	620.31	620.30	$6 \leftarrow 5$	691.42	691.47
$8 \leftarrow 7$	708.92	708.87	$7 \leftarrow 6$	806.78	806.65
$9 \leftarrow 8$	797.41	797.43	$8 \leftarrow 7$	921.70	921.79
$10 \leftarrow 9$	886.78	885.97	$9 \leftarrow 8$	1036.83	1036.91
$11 \leftarrow 10$	974.65	974.49	$10 \leftarrow 9$	1151.21	1151.98
$12 \leftarrow 11$	1063.00	1062.98	$11 \leftarrow 10$	1266.97	1267.01
$13 \leftarrow 12$	1151.47	1151.45	$12 \leftarrow 11$	1382.03	1381.99
$14 \leftarrow 13$	1239.98	1239.89	$13 \leftarrow 12$	1496.96	1496.92
$15 \leftarrow 14$	1328.28	1328.31	$14 \leftarrow 13$	1611.80	1611.79
$16 \leftarrow 15$	1416.72	1416.69	$15 \leftarrow 14$	H_2O	1726.60
$17 \leftarrow 16$	1505.18	1505.04	$16 \leftarrow 15$	1841.36	1841.34
$18 \leftarrow 17$	1593.44	1593.36	$17 \leftarrow 16$	1956.26	1956.02
$19 \leftarrow 18$	1681.48	1681.64	$18 \leftarrow 17$	H_2O	2070.61
$20 \leftarrow 19$	1769.88	1769.88	$19 \leftarrow 18$	2185.57	2185.13
$21 \leftarrow 20$	1858.26	1858.08	$20 \leftarrow 19$	2299.42	2299.57
$22 \leftarrow 21$	1946.44	1946.23			
$23 \leftarrow 22$	2034.25	2034.35			
$24 \leftarrow 23$	2122.45	2122.42			
$25 \leftarrow 24$	2210.48	2210.44			
$26 \leftarrow 25$	2298.20	2298.41			

Transitions obscured by water lines are marked H_2O.

at 1116.33 GHz and $14_{2,12} \leftarrow 15_{2,3}$ at 1117.13 GHz. Formaldehyde was only observed at low pressure ($P \leqslant 2$ mbar) as the molecule has a low vapour pressure and is hydrophilic so tends to condense onto the metallic surfaces of the sample chamber. The gas inside the sample chamber is saturated at a low formaldehyde concentrations, therefore due to the low line areas the transitions are only visible when the line widths are small. Ammonia (NH_3) is also expected to be present in cigarette smoke; however, despite its numerous intense rotational transitions in the THz region no lines were observed, thought to be caused by either condensation or reaction of the NH_3 prior to measurement.

4.2. Species quantification

Once identified the concentration of the absorbing species can be quantified by determining the line area of a single transition. The line area is obtained by fitting the measured transition profile to theoretical profile dependent broadening regime of the gas under measurement. Gases at low pressure, $P < 1$ mbar exhibit only a Doppler linewidth

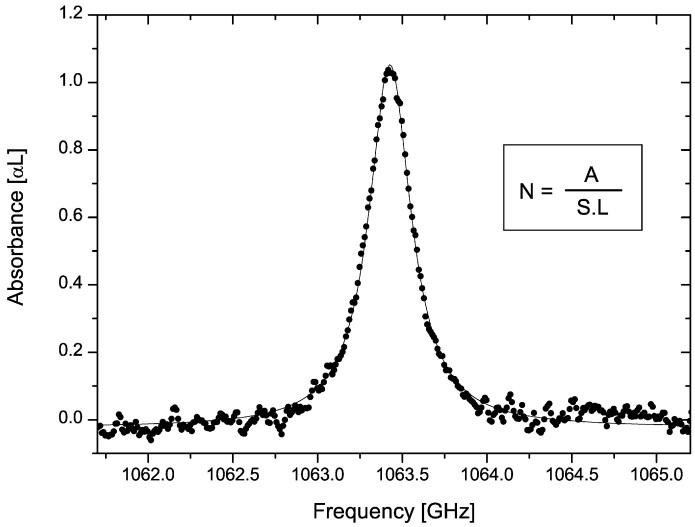

Fig. 10. Absorption spectrum of cigarette smoke containing the 12 ← 11 transition of HCN ($P = 38.4$ mbar, $T = 294$ K). Measured data (circles) and fitted Lorentzian function (line).

and are so fitted with a Gaussian function. At pressures in excess of 10 mbar the linewidth is dominated by molecular collisions so a Lorentzian profile can be applied. Intermediate pressures require both regimes to be accounted for, so a Voigt profile is used and is a convolution of the Gaussian and Lorentzian profiles. In the case of species concentration measurements of the cigarette smoke at pressures of 20 mbar the collisional broadening is very much greater than the Doppler width, for example HCN displays a collisional broadening (≈60 MHz, HWHM) some two orders greater than the Doppler width for HCN (≈1.2 MHz). A Lorentzian profile, Eq. (3), was applied to the measured spectra using a standard non-linear fitting technique yielding the line area A, the centre frequency ν_o, and the half width half maximum $\Delta\nu$, see Fig. 10. The species concentration N (molecules cm^{-3}) may be directly calculated using A, the interaction length L and the line intensity S. Tabulated values for transition line intensities of numerous species may be found in the literature or spectroscopy databases such as HITRAN [44], CDMS [45], NIST Physical Reference Data [46], JPL Molecular Spectroscopy catalog [47], and GEISA [48]. Species for which no information is available must be characterised by the measurement of calibrated gas samples.

$$\alpha(\nu).L = \frac{A}{\pi}.\left[\frac{\Delta\nu}{(\nu-\nu_o)^2+\Delta\nu^2}\right] \tag{3}$$

In a similar manner the spectral purity of the instrument is significantly narrower than the line widths hence is not accounted for during the data analysis. The HCN concentration determined for the 14 ← 13 transition was 210.3 ppm within the smoke mixture. In order to confirm the validity of this measurement and to establish comparisons with the existing literature on the composition of cigarette smoke the mass of HCN per cigarette was determined using a number of transitions, yielding a value of 160.1 ± 8.4 mg/cigarette. A study performed by the tobacco industry using an accepted sample preparation protocol and measurement by FTIR spectrometer obtained a mass of 200 ± 22 mg/cigarette, the difference between the values is thought to result from the sample preparation where combustion temperature and gas flow rates are critical. The strongly polar HCN molecule (3 Debye) is easily quantified by this technique, however, molecules with weaker dipole moments such as CO (0.1 Debye) which are found at higher concentrations in cigarette smoke also display sufficient absorption to allow their quantification. An identical procedure was adapted to multiple recordings of the 12 ← 11 and 14 ← 13 CO transitions to give a measured concentration of $1.7 \pm 0.3\%$ in the smoke, corresponding to a mass of 13 ± 2 mg/cigarette. More intense CO transitions can be found in the infra-red region and are used by commercially available instruments giving a comparative value of 18 ± 5 mg/cigarette for a smoke sample prepared under identical conditions or 12 ± 2 mg/cigarette for smoke generated according to protocol accepted by tobacco research [49]. However, this type of instrument requires the particles and moisture contained in the smoke to be removed by a heated dust filter prior to analysis [50]. The measurement of

CO by the CW-THz spectrometer was also validated by the use of standard commercially prepared and calibrated gas with good agreement between the gas calibration and measurement.

5. Conclusion

Laboratory studies of calibrated pure gas phase samples using a CW-THz spectrometer has been shown to yield parameters such as line intensity and self-broadening coefficients. Comparison of the measured line intensity with calculated and published values displays a good agreement and reveals the possibility of this technique to make independent absolute concentration measurements. These spectroscopic parameters are essential to the exploitation of this spectral region for detection of gases. The spectrometer has also demonstrated its ability to simultaneously identify multiple species in a complex subject. The species selectivity is achieved thanks to the measurement of pure rotational transitions of small strongly polar molecules. At pressures in the order of 10 mbar the lines rarely overlap and the observation of multiple transitions of a particular species can easily confirm its presence. The quantification is a straightforward procedure requiring the line intensity. The use of multiple lines for a single species can enable the measurement uncertainty to be reduced. An attractive possibility of this kind of measurement is the potential to make absolute concentration measurements independent of any experimental or inferred calibration. For example, the CW-THz spectrometer was able to confirm the presence of HCN in cigarette smoke by the observation of several isolated transitions. Its quantification resulted in a measurement uncertainty of 8 mg/cigarette, approximately half that obtained by FTIR currently employed for this kind of measurement. The complex mixture of species in the cigarette smoke containing many reactive compounds presents a difficult subject for the analytical chemistry techniques which have limited selectivity. In the case of CO the weaker dipole results in an uncertainty of 2 mg/cigarette identical to that obtained in existing tobacco research obtained by infra-red absorption which has the advantages of being a direct optical method but requires a pre-filtration to remove the particles which obscure the optical path. In comparison the CW-THz spectrometer was able to measure the unfiltered cigarette smoke as the longer wavelength radiation ($\lambda \approx 200$ μm) does not interact with the aerosols. The immunity of the THz radiation to scattering is of great advantage when measurements are to be made in a 'hostile' or visibly opaque environment such as smoke, flames, dust clouds, fog, sprays etc. Unfortunately to improve the spectrometer detection limit, photomixing devices capable of delivering higher power are required. At present, these components are limited by the thermal management of the GaAs substrate. An additional improvement can also be envisaged by increasing the interaction between the THz radiation and the gas under study. Potential solutions to this problem are the use of a multiple pass gas cell, a resonant measurement cell, or inclusion of the sample gas in a THz waveguide, however, the effective interaction length must always be known to permit quantification. The increased spectrometer sensitivity offered by these improvements should allow a larger variety of molecules to be measured particularly the less volatile species which are present only at low concentrations but have important roles in the chemistry of the atmosphere. The frequency resolution of the spectrometer is sufficient for the measurement of non-Doppler limited absorption profiles however the absolute frequency calibration is achieved using transitions at known frequencies, solutions to this problem are currently under investigation.

Acknowledgements

A particular thanks to Sophie Matton [39] and Damien Bigourd [43] both of whom completed a PhD on this subject. The authors would also like to thank Eric Fertein and Marc Fourmentin for their contributions to this work along with François Rohart (PhLAM), Karine Blary (IEMN) and Jean-François Lampin (IEMN) for their active collaborations. This work has been partially funded by the award of an Action de recherche concertée d'initiative régionale (ARCir) grant financed by the Conseil Régional Nord-Pas de Calais.

References

[1] G. Winnewisser, A. Krupnov, M. Tretyakov, M. Liedtke, F. Lewen, A. Saleck, R. Schieder, A. Shkaev, S. Volokhov, Precision broad-band spectroscopy in the terahertz region, Journal of Molecular Spectroscopy 165 (1) (1994) 294–300.

[2] M. Kreglewski, J. Cosleou, G. Wlodarczak, Rotational spectrum of hydrazine in the submillimeter range, Journal of Molecular Spectroscopy 216 (2) (2002) 501–504.

[3] D. Boucher, R. Bocquet, J. Burie, W. Chen, A far-infrared heterodyne side-band spectrometer, Journal de Physique III 4 (8) (1994) 1467–1480.

[4] G. Blake, K. Laughlin, R. Cohen, K. Busarow, D. Gwo, C. Schmuttenmaer, D. Steyert, R. Saykally, Tunable far infrared-laser spectrometers, Review of Scientific Instruments 62 (7) (1991) 1693–1700.
[5] P. Verhoeve, E. Zwart, M. Versluis, M. Drabbels, J. Termeulen, W. Meerts, A. Dymanus, D. Mclay, A far infrared-laser sideband spectrometer in the frequency region 550–2700 GHz, Review of Scientific Instruments 61 (6) (1990) 1612–1625.
[6] F. Lewen, E. Michael, R. Gendriesch, J. Stutzki, G. Winnewisser, Terahertz laser sideband spectroscopy with backward wave oscillators, Journal of Molecular Spectroscopy 183 (1) (1997) 207–209.
[7] P. Roy, M. Rouzieres, Z. Qi, O. Chubar, The AILES infrared beamline on the third generation synchrotron radiation facility SOLEIL, Infrared Physics and Technology 49 (1–2) (2006) 139–146.
[8] J. Ortega, F. Glotin, R. Prazeres, Extension in far-infrared of the CLIO free-electron laser, Infrared Physics and Technology 49 (1–2) (2006) 133–138.
[9] H. Hubers, S. Pavlov, H. Richter, A. Semenov, L. Mahler, A. Tredicucci, H. Beere, D. Ritchie, High-resolution gas phase spectroscopy with a distributed feedback terahertz quantum cascade laser, Applied Physics Letters 89 (6) (2006) 061115.
[10] D. Auston, Subpicosecond electrooptic shock-waves, Applied Physics Letters 43 (8) (1983) 713–715.
[11] D. Auston, K. Cheung, Coherent time-domain far-infrared spectroscopy, Journal of the Optical Society of America B—Optical Physics 2 (4) (1985) 606–612.
[12] L. Duvillaret, F. Garet, J. Coutaz, Highly precise determination of optical constants and sample thickness in terahertz time-domain spectroscopy, Applied Optics 38 (2) (1999) 409–415.
[13] L. Duvillaret, F. Garet, J. Coutaz, A reliable method for extraction of material parameters in terahertz time-domain spectroscopy, IEEE Journal of Selected Topics in Quantum Electronics 2 (3) (1996) 739–746.
[14] D. Mittleman, Sensing with Terahertz Radiation, Springer-Verlag, Berlin, 2003.
[15] Nikon, http://www.nikon.co.jp.
[16] Picometrix, http://www.picometrix.com/.
[17] TeraView Ltd.
[18] W. King, W. Gordy, One-to-two millimeter wave spectroscopy. IV. Experimental methods and results for OCS, CH_3F, and H_2O, Phys. Rev. 93 (1954) 407–412.
[19] R. Bocquet, G. Wlodarczak, A. Bauer, J. Demaison, The submillimeter-wave rotational spectrum of methyl cyanide—analysis of the ground and the low-lying excited vibrational-states, Journal of Molecular Spectroscopy 127 (2) (1988) 382–389.
[20] P. Helminger, J. Messer, F. Delucia, Continuously tunable coherent spectroscopy for the 0.1–1.0-THz region, Applied Physics Letters 42 (4) (1983) 309–310.
[21] C. Endres, H. Muller, S. Brunken, D. Paveliev, T. Giesen, S. Schlemmer, F. Lewen, High resolution rotation-inversion spectroscopy on doubly deuterated ammonia, ND2H, up to 2.6 THz, Journal of Molecular Structure 795 (1–3) (2006) 242–255.
[22] T. Crowe, W. Bishop, D. Porterfield, J. Hesler, R. Weikle, Opening the terahertz window with integrated diode circuits, IEEE Journal of Solid-State Circuits 40 (10) (2005) 2104–2110.
[23] K. Evenson, D. Jennings, F. Petersen, Tunable far-infrared spectroscopy, Applied Physics Letters 44 (6) (1984) 576–578.
[24] H. Odashima, L. Zink, K. Evenson, Tunable far-infrared spectroscopy extended to 9.1 THz, Optics Letters 24 (6) (1999) 406–407.
[25] E. Brown, K. Mcintosh, K. Nichols, C. Dennis, Photomixing up to 3.8-THz in low-temperature-grown GaAs, Applied Physics Letters 66 (3) (1995) 285–287.
[26] K. Mcintosh, E. Brown, K. Nichols, O. Mcmahon, W. Dinatale, T. Lyszczarz, Terahertz photomixing with diode lasers in low-temperature-grown GaAs, Applied Physics Letters 67 (26) (1995) 3844–3846.
[27] A. Pine, R. Suenram, E. Brown, K. Mcintosh, A terahertz photomixing spectrometer: Application to SO2 self broadening, Journal of Molecular Spectroscopy 175 (1) (1996) 37–47.
[28] H. Ito, F. Nakajima, T. Furuta, T. Ishibashi, Continuous THz-wave generation using antenna-integrated uni-travelling-carrier photodiodes, Semiconductor Science and Technology 20 (7) (2005) S191–S198.
[29] T. Goyette, W. Guo, F. Delucia, J. Swartz, H. Everitt, B. Guenther, E. Brown, Femtosecond demodulation source for high-resolution submillimeter spectroscopy, Applied Physics Letters 67 (25) (1995) 3810–3812.
[30] O. Pirali, N. Van-Oanh, P. Parneix, M. Vervloet, P. Brechignac, Far-infrared spectroscopy of small polycyclic aromatic hydrocarbons, Physical Chemistry Chemical Physics 8 (32) (2006) 3707–3714.
[31] V. Podobedov, D. Plusquellic, G. Fraser, THz laser study of self-pressure and temperature broadening and shifts of water vapor lines for pressures up to 1.4 KPa, Journal of Quantitative Spectroscopy and Radiative Transfer 87 (3–4) (2004) 377–385.
[32] P. Chen, J. Pearson, H. Pickett, S. Matsuura, G. Blake, Measurements of (nh3)-n-14 in the nu(2) = 1 state by a solid-state, photomixing, THz spectrometer, and a simultaneous analysis of the microwave, terahertz, and infrared transitions between the ground and nu(2) inversion–rotation levels, Journal of Molecular Spectroscopy 236 (1) (2006) 116–126.
[33] Institut d'electronique de microélectronique et de nanotechnologie, http://www.iemn.univ-lille1.fr/.
[34] E. Peytavit, S. Arscott, D. Lippens, G. Mouret, S. Matton, P. Masselin, R. Bocquet, J. Lampin, L. Desplanque, F. Mollot, Terahertz frequency difference from vertically integrated low-temperature-grown GaAs photodetector, Applied Physics Letters 81 (7) (2002) 1174–1176.
[35] G. Mouret, S. Matton, R. Bocquet, D. Bigourd, F. Hindle, A. Cuisset, J. Lampin, D. Lippens, Anomalous dispersion measurement in terahertz frequency region by photomixing, Applied Physics Letters 88 (18) (2006) 181105.
[36] K. Yamada, S. Klee, Pure rotational spectrum of H2S in the far-infrared region measured by FTIR spectroscopy, Journal of Molecular Spectroscopy 166 (2) (1994) 395–405.
[37] Laboratoire de physique des lasers, atomes et molécules, http://www-phlam.univ-lille1.fr/.
[38] S. Matton, F. Rohart, R. Bocquet, G. Mouret, D. Bigourd, A. Cuisset, F. Hindle, Terahertz spectroscopy applied to the measurement of strengths and self-broadening coefficients for high-J lines of OCS, Journal of Molecular Spectroscopy 239 (October 2006) 182–189.

[39] S. Matton, Generation de rayonnement terahertz par photomelange et developpement d'une detection homodyne. Application a la caracterisation de polluants atmospheriques et de milieux dielectriques, PhD thesis, Université du Littoral Côte d'Opale, 2004.
[40] R.C.W. Gordy, Microwave Molecular Spectra, John Wiley and Sons, New York, 1984.
[41] R. Weiss, Stark effect and hyperfine structure of hydrogen fluoride, Physical Review 131 (2) (1963) 659–665.
[42] R.R. Baker, Smoke chemistry, in: D.E.L. Davis, M.T. Nielsen (Eds.), Tobacco: Production, Chemistry and Technology, Blackwell Science, London, ISBN 0632047917, 1999.
[43] D. Bigourd, Etude et detection de polluants atmospheriques dans le domaine THz, PhD thesis, Universite du Littoral Cote d'Opale, 2006.
[44] L. Rothman, D. Jacquemart, A. Barbe, D. Benner, M. Birk, L. Brown, M. Carleer, C. Chackerian, K. Chance, L. Coudert, V. Dana, V. Devi, J. Flaud, R. Gamache, A. Goldman, J. Hartmann, K. Jucks, A. Maki, J. Mandin, S. Massie, J. Orphal, A. Perrin, C. Rinsland, M. Smith, J. Tennyson, R. Tolchenov, R. Toth, J. Vander Auwera, P. Varanasi, G. Wagner, The HITRAN 2004 molecular spectroscopic database, Journal of Quantitative Spectroscopy and Radiative Transfer 96 (2) (2005) 139–204, http://www.hitran.com.
[45] Cologne database for molecular spectroscopy, http://www.ph1.uni-koeln.de/vorhersagen/.
[46] National institute of standards and technology, http://physics.nist.gov/PhysRefData/MolSpec/index.html.
[47] Jet propulsion laboratory, http://spec.jpl.nasa.gov/.
[48] Gestion et étude des informations spectroscopiques et atmospheriques, http://ara.lmd.polytechnique.fr/htdocs-public/products/GEISA/HTML-GEISA/index.html.
[49] A. Calafat, G. Polzin, J. Saylor, P. Richter, D. Ashley, C. Watson, Determination of tar, nicotine, and carbon monoxide yields in the mainstream smoke of selected international cigarettes, Tobacco Control 13 (1) (2004) 45–51.
[50] N. Masalehdami, J. Potdevin, F. Cazier, D. Courcot, in: Int. Conf. on Coal Fire Research, 2005, pp. 101–103.